Order–Disorder Phenomena. III. Effect of Temperature and Pressure on the Elastic Constants of Ammonium Chloride

Carl W. Garland and Rémi Renard

Reprinted from The Journal of Chemical Physics, Vol. 44, No. 3, pp. 1130-1139, 1 February 1966

Reprinted from THE JOURNAL OF CHEMICAL PHYSICS, Vol. 44, No. 3, 1130–1139, 1 February 1966
Printed in U. S. A.

Order–Disorder Phenomena. III. Effect of Temperature and Pressure on the Elastic Constants of Ammonium Chloride*

CARL W. GARLAND AND RÉMI RENARD†
Department of Chemistry, Research Laboratory of Electronics, and Center for Materials Science and Engineering Massachusetts Institute of Technology, Cambridge, Massachusetts

(Received 18 August 1965)

The adiabatic elastic constants of single-crystal ammonium chloride have been measured at 20 Mc/sec as functions of temperature and pressure in the region of the lambda transition. At atmospheric pressure, data were obtained over the range of temperature from 150° to 320°K. At five temperatures, evenly spaced between 250° and 310°K, measurements were made as the pressure was varied from 0 to 12 kbar. The values at 300°K and atmospheric pressure are: $c_{11}=3.815$, $c_{44}=0.8878$, $C'=1.4698$, in units of 10^{11} dyn cm^{-2}. A hysteresis of the critical temperature, equal to $\sim$0.9°K at atmospheric pressure, was observed; this hysteresis disappears rapidly as the hydrostatic pressure is increased. The results are in good agreement with those predicted for a compressible Ising model. In particular, it is concluded that the order–disorder transition in ammonium chloride is not of a simple lambda type. It is proposed that NH_4Cl is unstable in the immediate vicinity of its critical point and undergoes a first-order transition.

INTRODUCTION

AMMONIUM chloride undergoes a lambda transition of the order–disorder type which involves the relative orientations of the tetrahedral ammonium ions in a CsCl-type structure. As a result of electrostatic attractions, the most stable orientation of the NH_4^+ ion in the cubic unit cell is for the hydrogen atoms to point toward the nearest-neighbor Cl^- ions. Thus there are two possible positions for the ammonium ion. In the completely ordered state, all NH_4^+ tetrahedra have the same relative orientation with respect to the crystallographic axes (at least for a given domain); in the completely disordered state, the orientations are random with respect to these two positions.[1] Strictly speaking, the NH_4^+ ions librate about their equilibrium positions in both the ordered and disordered state.[2]

In many respects NH_4Cl is an ideal crystal for studying cooperative order–disorder phenomena. The orientational ordering is of a simple kind, completely analogous to the spin ordering of a simple-cubic ferromagnet in zero external field. The difference in interaction energy between parallel and antiparallel NH_4^+ ions is very largely due to octopole–octopole terms between nearest NH_4^+ neighbors,[3] and thus the Ising model is quite a good approximation for a NH_4Cl lattice. Furthermore, the ordering process should have little effect on the dynamics of such an ionic lattice. For these reasons, the theory developed in the preceding papers[4,5] (called Papers I and II) for the mechanical behavior of an Ising lattice should be directly pertinent to an interpretation of the elastic properties of ammonium chloride.

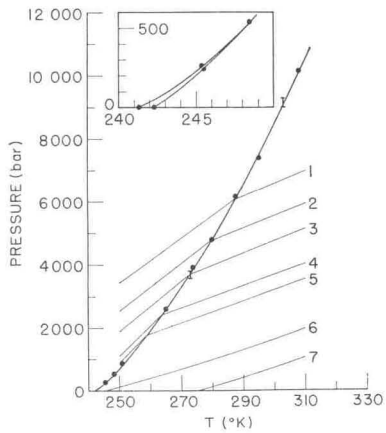

FIG. 1. Phase diagram for NH_4Cl. The high-pressure, low-temperature field corresponds to the ordered phase. The data points were obtained from the abrupt "break" in the ultrasonic shear velocities at the λ transition point (see Figs. 8 and 9); the vertical bars indicate static volume measurements of Bridgman.[17] The light lines numbered 1 through 7 represent isochores at various volumes (see legend of Fig. 5 for values of V_i).

The present paper reports the results of a variety of ultrasonic velocity measurements which have been made on single-crystal ammonium chloride. Both longitudinal and transverse acoustic waves were studied over a wide range of temperature (150°–320°K) and pressure (0 to 12 kbar). In these investigations special emphasis was given to the "anomalous" behavior near the lambda transition. As shown in Fig. 1, the transi-

* This work was supported in part by the Joint Services Electronics Program under Contract DA36-039-AMC-03200(*E*); and in part by the Advanced Research Projects Agency.

† Present address: Centre de Recherches, Esso Standard SAF, Mont St. Aignan (Seine Maritime), France.

[1] H. A. Levy and S. W. Peterson, Phys. Rev. **83,** 1270 (1951), **86,** 766 (1952).

[2] E. L. Wagner and D. F. Hornig, J. Chem. Phys. **18,** 296, 305 (1950).

[3] C. W. Garland and J. S. Jones, J. Chem. Phys. **41,** 1165 (1964).

[4] C. W. Garland and R. Renard, J. Chem. Phys. **44,** 1120 (1966)

[5] R. Renard and C. W. Garland, J. Chem. Phys. **44,** 1125 (1966).

tion temperature is a fairly strong function of pressure, increasing from ~242°K at 1 atm to ~308°K at 10 kbar. Ultrasonic velocities at a constant pressure of 1 atm have been measured previously[6] by a pulse-echo method as a function of frequency and temperature, and no dispersion was observed between 5 and 55 Mc/sec. The temperature dependence at 1 atm has been restudied, and the pressure dependence of the velocities were measured at five fixed temperatures spaced between 250° and 308°K. Thus, we have very precise velocity data on both the ordered and disordered phases. These experimental data will permit us to separate the effects on the elastic properties of changes in volume and changes in temperature from the effects due to changes in ordering (at constant V and T).

The results presented below are given in terms of the variation of the three adiabatic elastic constants c_{11}, c_{44}, and C', which can be obtained directly from the experimental sound velocities. Third-order elastic constants are not used, and for pressures above 1 atm the quantities c_{11}, c_{44}, and C' are "effective" elastic constants.[7] The relations between the ultrasonic velocities and the elastic constants of a cubic crystal are well known:

$$c_{11}=\rho U_l^2, \tag{1}$$

where ρ is the mass density of the crystal and U_l is the velocity of a longitudinal sound wave traveling in the [100] direction;

$$c_{44}=\rho U_t^2, \tag{2}$$

where U_t is the velocity of a transverse wave traveling in the [100] direction and polarized in any direction;

$$C'=(c_{11}-c_{12})/2=\rho U_{t'}^2, \tag{3}$$

where $U_{t'}$ is the velocity of a transverse wave traveling in the [110] direction and polarized perpendicular to the [001] axis;

$$c_{11}+c_{44}-C'=\rho U_{l'}^2, \tag{4}$$

where $U_{l'}$ is the velocity of a longitudinal wave traveling in the [110] direction. Values of $U_{l'}$ were measured only at 1 atm as a check on the internal consistency of the data.

EXPERIMENTAL WORK

In order to achieve both a very good absolute accuracy and an excellent relative precision for all the velocities, measurements were made with the pulse-superposition technique. This method, developed by McSkimin,[8,9] involves applying identical external pulses to the sample at a repetition rate $N=1/t$ such that t is approximately equal to some integral multiple (p) of the time delay between successive echoes. When the value of t is slowly varied, the amplitude of the superposed echoes will oscillate between a maximum value corresponding to all echoes being in phase and a minimum value corresponding to successive echoes being out of phase. The general expression for an *in-phase* value of t is given by[8,9]

$$t=p\delta-p\gamma/360f+n/f, \tag{5}$$

where $t(=1/N)$ and the rf carrier frequency f are known by direct measurement, p is an exact integer determined by the mode of operation, and $\delta=2L/U$ is the true round-trip transit time for a plane sound wave with velocity of propagation U traveling back and forth inside a sample of length L. In order to determine δ one must evaluate γ, the phase shift (in degrees) associated with the reflection of the sound wave at the transducer+seal end of the sample, and the integer n which indicates which of the in-phase conditions is involved. (For $n=0$, the first rf peaks of all the superposed echoes coincide; for $n=\pm1$ the first peaks of successive superposed echoes are displaced by one period of the carrier frequency, etc.) The value of γ can be calculated[8] from the acoustical impedances of the sample, seal, and transducer, the thicknesses of the seal and transducer, and the frequency f. All of these quantities are known with sufficient accuracy except the seal thickness. In order to determine the seal thickness and the n values, in-phase values of t were determined at two different frequencies—f_R, the resonance frequency of the transducer, and a second frequency between $0.90f_R$ and $0.95f_R$. Although the pulse-superposition method is experimentally and computationally more difficult than the pulse-echo method, it has the great advantage of involving the measurement of a frequency rather than of a time delay and of allowing one to evaluate quantitatively the effect of reflections. Further refinements of this method are given in a recent paper by McSkimin.[10] The only disadvantage of this method for the present investigation is the fact that it cannot be used under conditions where the sample has a very large ultrasonic absorption.

All of the measurements were carried out in the $p=1$ mode of operation since this is the best method for the unambiguous determination of the $n=0$ value of t. In order to observe the superposed echo signals in this case it is necessary to interrupt the sequence of external pulses. This is easily achieved by using the A^+ gate of a Tektronix 545A oscilloscope to block the generation of external pulses during the time of the A sweep. A block diagram of the electronic circuit is shown in Fig. 2; although equivalent to the original McSkimin setup, the present apparatus involves differ-

[6] C. W. Garland and J. S. Jones, J. Chem. Phys. **39**, 2874 (1963).
[7] R. N. Thurston, J. Acoust. Soc. Am. **37**, 348 (1965).
[8] H. J. McSkimin, J. Acoust. Soc. Am. **33**, 12 (1961).
[9] H. J. McSkimin and P. Andreatch, J. Acoust. Soc. Am. **34**, 609 (1962); J. Appl. Phys. **34**, 651 (1963).
[10] H. J. McSkimin, J. Acoust. Soc. Am. **37**, 864 (1965).

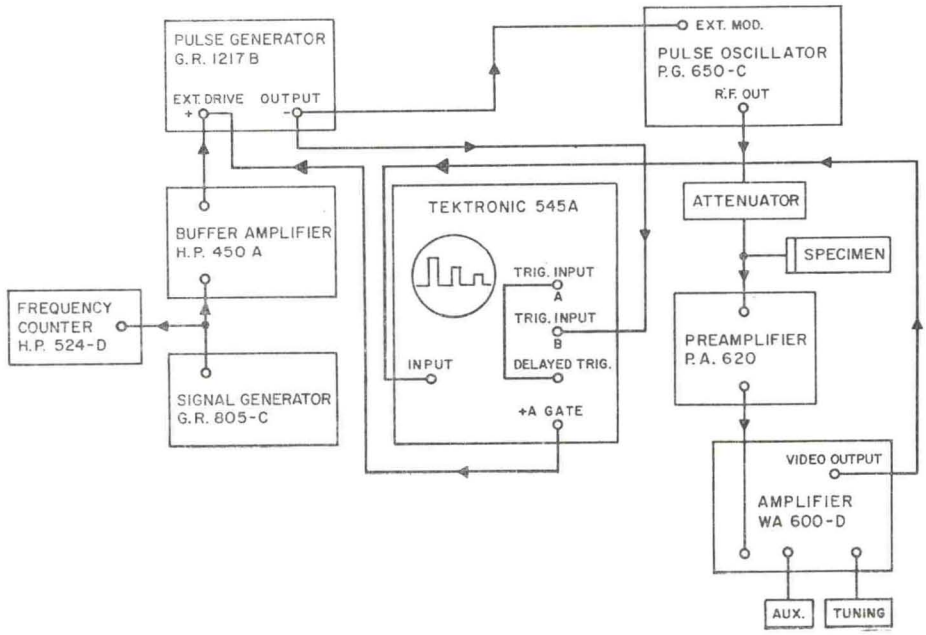

FIG. 2. Block diagram of the electronic circuit used in the pulse superposition method.

ent components. The only special equipment is the pulsed oscillator, which is a modified version of an Arenberg PG-650C oscillator. After modification, this generator can now produce rectangular-shaped, rf-modulated pulses of a duration up to 3 μsec at a maximum triggering rate of 200 kc/sec.[11]

The single crystals used for these velocity determinations were grown from saturated solutions of ammonium chloride; the details of the process have been described previously.[6] When the crystals had two flat and smooth natural faces no special preparation was needed for measurements in the [100] direction. Otherwise, two faces were cut perpendicular to the desired direction of propagation, and these faces were polished to optical quality. Four crystals were used: Crystals A, B, and C for measurements in the [100] direction, and crystal D for measurements in the [110] direction. The lengths (L) as measured with a light-wave micrometer at 23°C were (A) 1.8300±0.0001 cm; (B) 1.6453±0.0001 cm; (C) 0.9239±0.0001 cm, and (D) 1.2056±0.0001 cm. After almost every run the seal had to be changed, otherwise the quality of the echoes deteriorated. As a result of these changes the faces were slowly damaged and the path lengths were slightly decreased. Periodic length measurements were made and correction factors were applied.

A density of 1.52637 g cm^{-3} at 296°K was calculated from a lattice constant of 3.8750 Å, which is based on x-ray measurements around room temperature.[12] The path length ratio at 1 atm $L(T)/L(296°\text{K})$ was calculated from the thermal expansion data compilated by Sakamoto[13] and from the low-temperature x-ray data of Vegard and Hillsund.[14] Smooth-curve values of this ratio are given in Table I.

For measurements as a function of pressure at constant temperature, it is convenient[15] to introduce another path-length ratio $s=L_1/L_p$, where L_1 is the sample length at a given temperature and 1 atm and L_p is the length at the same temperature under an external applied pressure p. The calculation of $s(p)$ requires a knowledge of the isothermal compressibility as a function of pressure. At low pressures (i.e., in the disordered phase away from the lambda line) our present adiabatic measurements can be used to obtain an excellent approximation to $s(p)$. However, the difference between the isothermal and adiabatic compressibilities becomes very large in the transition region,[16] and it is necessary to make use of isothermal data for obtaining $s(p)$ values above the critical pressure. Bridgman[17] has directly measured the pressure dependence at 273° and 303°K of the length of a polycrystalline pressed rod of ammonium chloride. Comparison between Bridgman's data and ours at low pressures indicates that his values of $s(p)$ are systematically high by about 10% over a wide range of pressure. Thus, we have chosen $s(p)$ values at 273° and 303°K by correcting Bridgman's values with a constant multiplicative factor: $s-1=0.9(s_B-1)$. Values of $s(p)$ at other temperatures were chosen by extrapolating our low pressure

[11] This modification of the Arenberg pulsed oscillator (PG-650C-mod. 5-2) can now be obtained commercially from Arenberg Ultrasonic Laboratory, 94 Green Street, Jamaica Plains, Massachusetts.

[12] R. W. G. Wycoff, *Crystals Structures* (Interscience Publishers, Inc., New York, 1964), Vol. 1, Chap. III.

[13] Y. Sakamoto, J. Sci. Hiroshima Univ. **A18,** 95 (1954).

[14] L. Vegard and S. Hillesund, Avhandl. Norske Videnskaps-Akad. Oslo, I. Mat. Naturv. Kl. No. 8 (1942); see Chem. Abs. **38,** 4488[8] (1944).

[15] R. K. Cook, J. Acoust. Soc. Am. **29,** 445 (1957).

[16] L. Tisza, Ann. Phys. (N.Y.) **13,** 1 (1961).

[17] P. W. Bridgman, Phys. Rev. **38,** 182 (1931).

values in a manner consistent with the corrected Bridgman curves. A plot of the $s(p)$ values adopted at various temperatures is shown in Fig. 3. Note that s varies by less than 2% over the pressure range involved in these experiments; thus a relative error of 5% in the extrapolation procedure will affect the value of s (and therefore the elastic constants) by only 0.1%.

Hydraulic pressure equipment of a conventional design was obtained from the Harwood Engineering Company, Walpole, Massachusetts. Pressures in excess of 12 kbar could be generated in the high-pressure cell, which was filled with a mixture of one-part Univis P38 oil and three-parts pure gasoline. The pressure values were determined from changes in the resistance of a calibrated manganin coil, which forms one arm of an equal-ratio dc Wheatstone bridge. Pressures could be measured with an accuracy of ±3 bar and could be maintained constant to within ±3 bar over a period of 60 min. The high-pressure cell was immersed in a regulated temperature bath, which could be kept constant to within ±0.05°C at any temperature between −30° and +50°C.

Measurements at 1 atm were made in a regulated temperature bath similar to that described by Lawson.[18] In essence, this consisted of a glass Dewar filled with methyl cellosolve, which could be cooled by circulating cold methanol through a copper coil. The temperature could be controlled to within ±0.05°K at any value within the range from 215° to 320°K. Below 215°K, cooling was achieved with cold nitrogen gas by using an apparatus described previously.[6] Sample temperatures were measured with a copper–constantan thermocouple.

For the measurements made at 1 atm, a variety of seal materials were used to cement the quartz transducer to the sample crystal. Dow resin 276-V9 seals were used between 242° and 320°K since McSkimin[8,19] has determined the acoustical impedances and their temperature dependences for this material. Unfortunately, such seals break at the critical temperature on cooling. Measurements can be made down to about 195°K by using Apiezon N as a seal. Comparison between data obtained above the transition temperature using Apiezon and Dow resin seals allows one to determine the phase-shift correction for these Apiezon seals. Nonaq stopcock grease was used to obtain data below 200°K, but it did not make as good a seal. Since the phase-shift correction term $\gamma/360f$ in Eq. (5) was always less than 0.02% at room temperature, it was possible to neglect the temperature dependence of γ without causing a serious error in the values calculated for the elastic constants at low temperatures.

For the measurements made at high pressures, it was necessary to use a seal which was insoluble in the hydraulic fluid. A suitable sealing material was found to be a polymer made by heating an equimolar mixture of phthalic anhydride and glycerine and then removing the water by vacuum distillation. All measurements were carried out at a rf frequency equal to the resonance frequency of a transducer at 1 atm. Thus, the phase angle γ will vary with pressure for two reasons: (a) the acoustical characteristics of the seal material vary and (b) the resonance frequency of the transducer varies. The effect of pressure on the seal is not known and has been neglected; the effect of pressure on the behavior of quartz transducers is known[9] and has been used to calculate γ as a function of pressure.

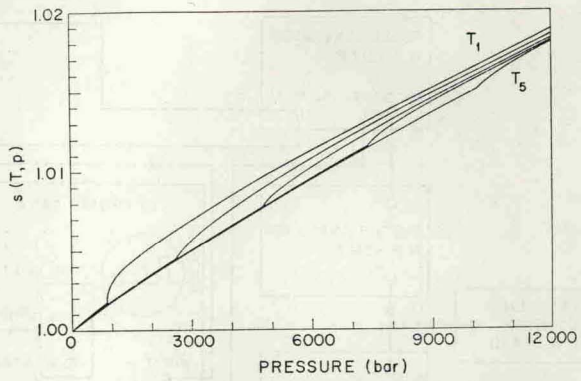

FIG. 3. Path length ratio s as a function of pressure for temperatures $T_1=250.72$°K; $T_2=265.00$°K; $T_3=280.05$°K; $T_4=295.02$°K; $T_5=308.04$°K.

RESULTS

Constant-Pressure Data

Experimental data points are shown in Figs. 4, 5, and 6 for the elastic constants c_{11}, c_{44}, and C' as functions of temperature at 1 atm. Each of these points was obtained directly from a single measurement of the propagation velocity of sound waves modulated at 20 Mc/sec; see Eqs. (1)–(3). Measurements were also performed at 60 Mc/sec in the temperature range $220°<T<300$°K, and those values agree with these 20 Mc/sec values within the limits of error. This absence of dispersion is in agreement with previous measurements[6] between 5 and 55 Mc/sec.

Because of the strong attenuation of longitudinal waves in the vicinity of the critical point, it was not possible to use the pulse-superposition method to measure c_{11} between 237° and 244°K. Instead, the variation of c_{11} in this temperature range was based on data obtained previously with a pulse-echo method.[6] Those older data now appear to have been subject to a systematic error and require correction. They have been corrected by adding a constant (temperature independent) value of 0.120×10^{11} dyn cm^{-2} to all the previous data points; this yields agreement with our present data below 237° and above 244°K.

Shear waves were not attenuated strongly at any temperature inside the investigated range; however,

[18] A. W. Lawson, Phys. Rev. **57**, 417 (1940).
[19] H. J. McSkimin, IRE (Inst. Radio Eng.) Trans. Ultrasonics Eng., PGUE-5, 25 (1957).

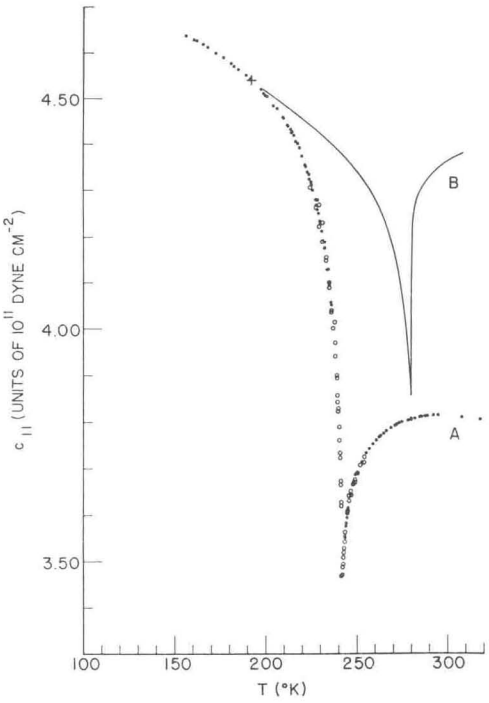

FIG. 4. Variation of c_{11} with temperature. Curve A: data at one atmosphere (solid circles are present measurements, open circles are corrected pulse-echo data[6]). Curve B: calculated curve at constant volume $V_2=34.15$ cm^3 mole^{-1}; V_2 corresponds to V_λ at 280°K and to the volume at 1 atm and 191.25°K (marked by cross).

hysteresis was observed in the critical region. Both c_{44} and C' increased gradually as the temperature was decreased until at 241.4°±0.1°K they suddenly showed a very large increase. At this temperature a new equilibrium was reached only after waiting for about 45 min. During this time c_{44} had suffered a jump of about +3.6% and C' a jump of about +1.2%. On further cooling the variation of these elastic constants was again smooth and gradual. Starting from a low temperature (say 220°K) and warming the sample, an

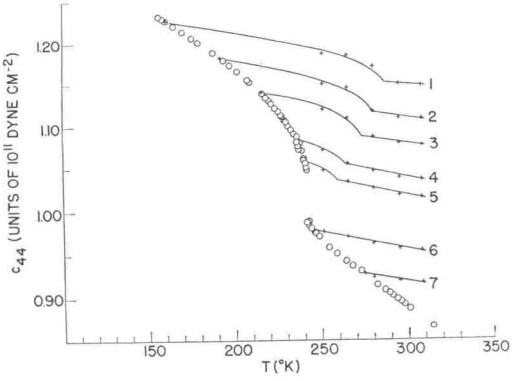

FIG. 5. Variation of c_{44} with temperature. Open circles are experimental data at 1 atm. Curves 1, 2, •••, 7 are calculated for various constant volumes: $V_1=34.002$; $V_2=34.150$; $V_3=34.266$; $V_4=34.428$; $V_5=34.507$; $V_6=34.768$; $V_7=34.928$ cm^3 mole^{-1}.

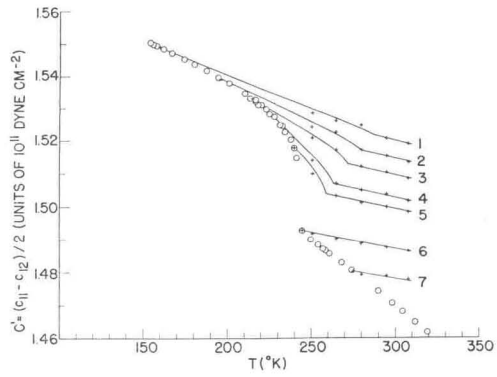

FIG. 6. Variation of C' with temperature. See legend of Fig. 5.

abrupt drop in the values of c_{44} and C' occurred at 242.3°±0.1°K, and a new equilibrium was again reached only after waiting for about 45 min. Below 241.4°K and above 242.3°K experimental values of the elastic constants were the same on cooling and on warming. This hysteresis loop has not been represented on Figs. 5 and 6 because the scale is too small to allow a clear representation of the phenomenon. The strong attenuation of longitudinal waves in the critical region prevented any such observation for c_{11}.

Presented in Table I is a tabulation of smooth-curve values of the experimental results at various temperatures in the range covered in these experiments. Note that values are given at 242.5°K rather than 242°K to avoid the region very close to the critical point which corresponds to a region of hysteresis.

An error analysis indicates that the maximum *random* error in these directly measured elastic quantities is 0.05% at room temperature. The error may be slightly

TABLE I. Smooth-curve values at one atmosphere for the adiabatic elastic constants c_{11}, c_{44}, and $C'=(c_{11}-c_{12})/2$, in units of 10^{11} dyn cm^{-2}. The adopted values of $L(T)/L(296°K)$ are also listed. The c_{11} entries marked by an asterisk are based on corrected data from a previous pulse-echo investigation.[6]

T(°K)	$L(T)/L(296°K)$	c_{11}	c_{44}	C'
155	0.98975	4.6402	1.2316	1.5499
170	0.99043	4.6086	1.2117	1.5462
190	0.99136	4.5473	1.1833	1.5411
210	0.99231	4.4532	1.1499	1.5349
230	0.99353	4.2235	1.1016	1.5260
250	0.99767	3.6892	0.9669	1.4902
270	0.99864	3.7890	0.9328	1.4819
290	0.99967	3.8138	0.9030	1.4738
310	1.00078	3.8117	0.8728	1.4657
236	0.99422	4.055	1.0804	1.5218
237	0.99437	4.008*	1.0758	1.5209
238	0.99452	3.955*	1.0712	1.5198
239	0.99468	3.887*	1.0656	1.5185
240	0.99487	3.813*	1.0592	1.5171
241	0.99508	3.734*	1.0515	1.5152
242.5	0.99724	3.507*	0.9830	1.4937
243	0.99728	3.538*	0.9818	1.4935
244	0.99734	3.582*	0.9796	1.4930
245	0.99739	3.609	0.9775	1.4925

larger at temperatures below the lambda point due to an increased uncertainty in the path-length correction. To check this figure we measured the quantity $(c_{11}+c_{44}-C')$ by exciting a longitudinal wave in the [110] direction; see Eq. (4). The experimental data were compared to the values calculated from the directly-measured elastic constants. The values agreed almost exactly at room temperature. For lower temperatures, the difference was always less than 0.16% in the disordered phase and it never exceeded 0.25% in the ordered phase.

The estimation of systematic errors is more difficult. In the pulse-superposition method an error of $|\Delta n|=1$ in the attribution of the n values to the in-phase conditions would lead to systematic errors greater than 1% in the elastic constants. We tried to prevent such mistakes by using several crystals of different lengths. With Crystals A and B we obtained excellent agreement (within the limits of random error) for the c_{11} values at room temperature. With Crystals B and C the agreement of c_{44} values was not as good: a relative deviation $[c_{44}(\mathrm{B})-c_{44}(\mathrm{C})]/c_{44}(\mathrm{B})=0.4\%$ was observed over the entire range of temperatures. The cause of this disagreement is unknown; it is not due to a misalignment of the crystal axes, a wrong attribution of the n values, or to diffraction effects. We have reported the values obtained with Crystal B since it had natural (100) faces and had not been cut or polished, but these c_{44} values may possible be systematically high by 0.4%.

TABLE II. The adiabatic elastic constants of ammonium chloride single crystals obtained from the present measurements (P) compared with the results obtained by Garland and Jones (G and J), by Haussuhl (H), and by Roa and Balakrishnan (R and B). All values are given in units of 10^{11} dyn cm^{-2}.

Obs.	T(°K)	c_{11}	c_{44}	C'
P	300	3.815	0.8878	1.4698
G and J	300	3.70	0.86	1.41
H	293	3.79	0.83	1.41
R and B	298	3.90	0.68	1.59
P	200	4.507	1.1674	1.5382
G and J	200	4.354	1.122	1.480

The adiabatic elastic constants of single-crystal ammonium chloride have been measured at room temperature by Haussuhl[20] and by Roa and Balakrishnan.[21] They have also been measured over the same range of temperatures as in the present work by Garland and Jones.[6] Table II gives a comparison of the values obtained by these various investigators with the results of the present experiments. It is striking that the present results are systematically 3% to 4% higher than those of Garland and Jones over the entire range of temperatures investigated. They used a pulse-echo method with unrectified pulses and determined the delay times by ranging the position of the rf peaks for a set of successive echoes. An examination of their data indicates that a systematic change in the delay times by a small number of rf periods would explain the discrepancy in most cases.

[20] S. Haussuhl, Acta Cryst. **13,** 685 (1960).

[21] R. V. G. Sundara Roa and T. S. Balakrishnan, Proc. Indian Acad. Sci. **A28,** 480 (1948).

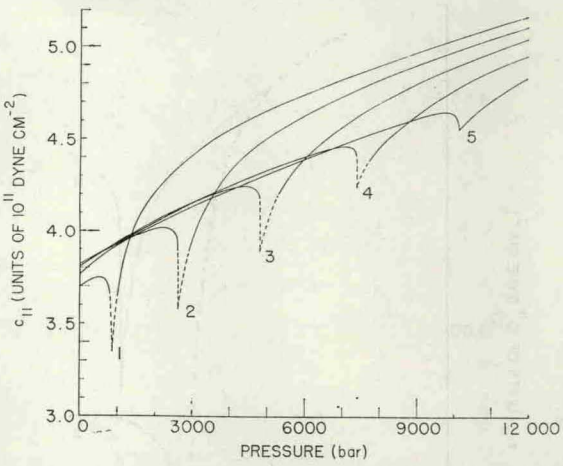

FIG. 7. Dependence of c_{11} on pressure at various temperatures (see Fig. 3 legend). Dashed portions of the curves indicate regions where data are less accurate or are missing due to high attenuation.

Constant-Temperature Data

Shown in Figs. 7, 8, and 9 are the pressure dependences of the effective adiabatic elastic constants c_{11}, c_{44}, and C'. These curves were calculated[15] from the known elastic constants at 1 atm, the adopted path length ratio s (see Fig. 3), and the experimental ratio N_p/N_1, where N_p is the $n=0$ repetition rate under an applied pressure p and N_1 is the value at 1 atm. All the data at high pressure were obtained at 20 Mc/sec. Although data points are not shown on these figures, each isotherm is based on at least 30 experimental points which show very little scatter. A tabulation of the smooth-curve values of experimental results over the range 0 to 12 kbar is presented in Table III.

Because of the strong attenuation of longitudinal waves in the critical region, it was not possible to

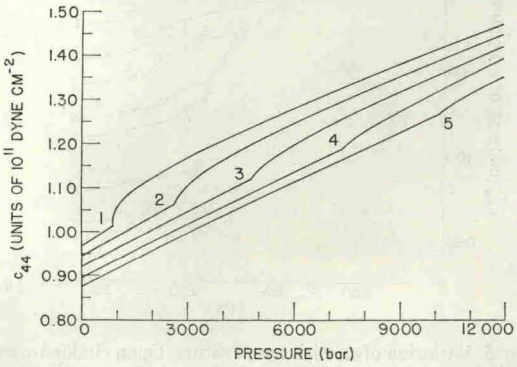

FIG. 8. Dependence of c_{44} on pressure at various temperatures (see Fig. 3 legend).

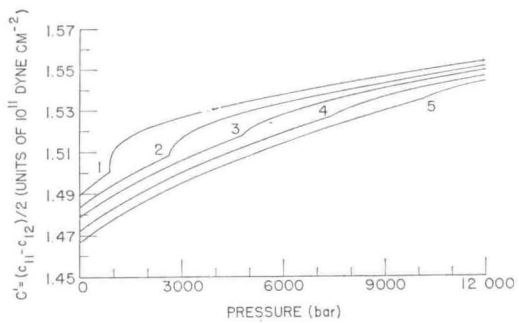

FIG. 9. Dependence of C' on pressure at various temperatures (see Fig. 3 legend).

determine c_{11} at pressures near the critical value except at T_5. For the other temperatures, smooth curves were rather arbitrarily drawn in the critical region. Shear waves are not attenuated; therefore the complete pressure dependence of c_{44} and C' could be studied. In measuring the velocity of shear waves we looked for hysteresis near the lambda line. No hysteresis was observed for any of the temperatures T_1, T_2, $\cdots$, T_5. We then made special runs at lower temperatures for the shear wave corresponding to c_{44}. At 245.42°K a hysteresis in pressure of about 30 bar was observed. At 248.41°K this hysteresis had disappeared. The hysteresis shown in Fig. 1 is based on these c_{44} data and the previously mentioned shear velocities at atmospheric pressure.

The application of a pressure to the crystal does not introduce any new source of errors which are not present for atmospheric-pressure measurements. However, the seal corrections are less and less accurate as the pressure increases because we do not know the characteristics of the seal under pressure. As a result, the random error in the elastic constants is of the order of $\pm 0.05\%$ at low pressure, but the uncertainty increases as the pressure increases. Both c_{11} and c_{44} have a fairly large pressure dependence which minimizes the importance of changes in the seal on the pressure derivative $d\ln c/dp$. Since C' varies only slowly with pressure, the error in $d\ln C'/dp$ could be much larger especially at higher pressures.

Constant-Volume Data

From the data presented above it is possible to get several new pieces of information. Combining the known temperature dependence of the length of the unit cell at atmospheric pressure, and the pressure dependence of s it was possible to compute the pressure which must be applied to the crystal to keep its volume constant. We did this for the following different values of the volume: $V_1=34.002$; $V_2=34.150$; $V_3=34.266$; $V_4=34.428$; $V_5=34.507$; $V_6=34.768$; $V_7=34.928$ cm^3 mole^{-1}. The corresponding p–T isochores are plotted in Fig. 1, which also shows the critical pressure p as a function of temperature. With these isochores we could evaluate the effective adiabatic elastic constants at constant volume. In Figs. 5 and 6 we have plotted the temperature dependence of c_{44} and C' at V_1, V_2, $\cdots$, V_7. The crosses correspond to the values obtained from data at T_1, T_2, $\cdots$, T_5. To avoid confusion on Fig. 4 we have plotted the temperature dependence of c_{11} only at volume V_2. These constant-volume plots are very important from a theoretical point of view because the theories of order–disorder phenomena are usually valid at constant volume and not at constant pressure.

DISCUSSION

The temperature–pressure region near the lambda line is of primary theoretical interest in the present work. Data obtained far from the transition region can be interpreted in terms of a crystal which is completely ordered or completely disordered. Observations of this kind on ammonium chloride are discussed elsewhere in connection with comparable data on the disordered phase of ammonium bromide.[22] We only point out here that, away from the lambda line, the elastic behaviors of the ordered and of the disordered crystal are essentially normal and very similar to each other. In previous papers,[6,23] the temperature dependence of the elastic constants at 1 atm near a lambda point has been discussed in terms of phenomenological Pippard

TABLE III. Smooth-curve values of the effective adiabatic elastic constants c_{11}, c_{44}, and C', in units of 10^{11} dyn cm^{-2}, as a function of temperature and pressure. $T_1=250.72$°K; $T_2=265.00$°K; $T_3=280.05$°K; $T_4=295.02$°K; $T_5=308.04$°K.

p (kbar)	T_1	T_2	T_3	T_4	T_5
			c_{11} values		
2	4.206	4.009	4.054	4.043	4.032
4	4.547	4.318	4.227	4.242	4.221
6	4.740	4.623	4.394	4.402	4.389
8	4.896	4.818	4.692	4.453	4.544
10	5.035	4.972	4.888	4.765	4.635
12	5.166	5.111	5.045	4.955	4.836
			c_{44} values		
2	1.1219	1.0335	1.0041	0.9773	0.9568
4	1.2065	1.1621	1.0867	1.0563	1.0353
6	1.2782	1.2453	1.1961	1.1353	1.1124
8	1.3457	1.3172	1.2800	1.2262	1.1869
10	1.4121	1.3852	1.3521	1.3155	1.2622
12	1.4742	1.4511	1.4238	1.3964	1.3536
			C' values		
2	1.5212	1.5032	1.4982	1.4919	1.4870
4	1.5308	1.5245	1.5127	1.5069	1.5017
6	1.5377	1.5336	1.5280	1.5189	1.5139
8	1.5438	1.5401	1.5372	1.5314	1.5249
10	1.5490	1.5461	1.5438	1.5407	1.5346
12	1.5540	1.5516	1.5495	1.5467	1.5442

[22] C. W. Garland and C. F. Yarnell, J. Chem. Phys. **44**, 1112 (1966).

[23] C. W. Garland, J. Chem. Phys. **41**, 1005 (1964).

equations. The discussion below is given in terms of the elastic behavior of an Ising model.

The two preceding papers[4,5] present an analysis of the mechanical properties of an Ising model. Paper I is concerned with an instability very close to the critical point and the resulting hysteresis which may occur in many properties. Leaving aside for the moment this important but relatively narrow range where instability may occur, it is possible to discuss the effect of ordering at constant volume on the elastic constants of an Ising model. We have carried out a general stress–strain analysis of the two-dimensional Ising lattice in Paper II and have obtained explicit formulae for the isothermal stiffnesses c_{11}, c_{44}, and $C'=(c_{11}-c_{12})/2$.

Now the order–disorder transition in ammonium chloride can be represented to a very good approximation by an Ising model of a simple-cubic ferromagnet. Although no exact solution of the three-dimensional Ising problem is yet available, the formal calculation of the elastic properties of a simple-cubic lattice will lead to results very similar to those for a square lattice. We see from Eqs. (41), (43), and (55) of Paper II that the constant-volume elastic properties of a cubic Ising lattice can be represented by

$$\frac{1}{\beta^T}\equiv c_{11}{}^T-(\tfrac{4}{3}C')=\frac{1}{\beta_{dl}{}^T}-\frac{vT}{J^2}\frac{C_I(0,\mathrm{H})}{N}\left(\frac{dJ}{dv}\right)^2 +\frac{v}{J}\frac{U_I(0,H)}{N}\left(\frac{d^2J}{dv^2}\right), \quad (6)$$

$$C'=C_{dl}'-mG(0,H)-nU_I(0,H)/NJ, \quad (7)$$

$$c_{44}=c_{44,dl}-lU_I(0,H)/NJ, \quad (8)$$

where $C_I(0,\mathrm{H})/N$ and $U_I(0,\mathrm{H})/N$ are the configurational heat capacity per "spin" and the Ising internal energy per "spin" as a function of $H\equiv J/kT$, J is the interaction energy between nearest-neighbor NH_4^+ ions, $G(0,H)$ is the three-dimensional analog of the function defined by Eq. (38) of Paper II, and v is the unit cell volume (which replaces σ, the area per spin, used in Paper II). The isothermal character of the reciprocal compressibility $1/\beta^T$ and the compressional stiffness $c_{11}{}^T$ is denoted by a superscript T; this is not necessary for the shear constants c_{44} and C' since the isothermal and adiabatic values are identical. The subscript dl indicates a disordered-lattice contribution (see Paper I for details) which corresponds to the essentially normal variations observed at temperatures far above T_λ. The coefficients m, n, and l are temperature-independent quantities, defined by Eqs. (39), (40), and (55) of Paper II except that σ must be changed to v.

For ammonium chloride, the parameter J is positive but dJ/dv and d^2J/dv^2 are negative with $|d^2J/dv^2|\ll|dJ/dv|$. Thus, we see from Eqs. (39) and (40) of II that both m and n are positive. The sign of l is not known since $\partial^2J/\partial\theta^2$ is unknown (θ is the angle by which the equilibrium angle of the cubic unit cell is istorted), but Eq. (55) and the accompanying discussion in Paper II make it physically reasonable that l is also positive.

The three-dimensional behavior of $U_I(0,H)$ and $G(0,H)$ is not known, but it will be generally similar to that found in two dimensions. A plot of $-U_I/NJ$ and $-G$ as a function of temperature is given in Paper II for the two-dimensional case. Note that $(-U_I)$ is zero in the completely disordered lattice and positive in the ordered lattice, while $(-G)$ is zero in both the completely ordered and completely disordered state but negative in the region of the transition. Both quantities are finite and continuous at all temperatures but have an inflection point of infinite slope at T_λ. In three dimensions, one would expect a sharpening of the variation above T_λ but no drastic changes.

Thus, we can predict from Eqs. (7) and (8) the qualitative behavior of the shear constants c_{44} and C'. Both "disordered-lattice" contributions should show a slow, smooth (almost linear) increase as the temperature is decreased; this is based on the behavior of any normal ionic crystal. The term $-lU_I(0,H)/NJ$ in Eq. (8) increases from zero in the completely disordered state to a constant positive value at temperatures quite a bit below T_λ. This increase is especially rapid as the temperature is decreased through the lambda point (which depends on the volume since J is a function of V). The constant-volume c_{44} curves in Fig. 5 show excellent agreement with this prediction. Indeed, the shape of these curves is what one would expect from an internal energy curve. The elastic constant C' should have qualitatively the same behavior as c_{44}, although they are not identical because Eq. (7) contains the term $-mG(0,H)$. Figure 6 does show that the temperature variation of C' at constant volume is similar to that of c_{44} although the effect of ordering is much smaller for C' and the shape of the curve changes with volume.

In order to discuss c_{11}, let us consider the appropriate linear combination of Eqs. (6) and (7). Since the configurational heat capacity has a sharp maximum at T_λ, the term $-(vT/J^2)(C_I/N)(dJ/dv)^2$ will dominate the temperature dependence of $c_{11}{}^T$. Hence $c_{11}{}^T$ should display a very pronounced minimum at the lambda point. From ultrasonic data we obtain $c_{11}{}^S$ rather than $c_{11}{}^T$, but these are related by

$$c_{11}{}^S=c_{11}{}^T+9\alpha^2VT/C_v(\beta^T)^2, \quad (9)$$

where α is the linear coefficient of thermal expansion. Although these isothermal and adiabatic stiffnesses differ considerably very close to T_λ, the difference between $c_{11}{}^T$ and $c_{11}{}^S$ is less than 10% when $|T-T_\lambda|\sim1°\mathrm{K}$ and this difference decreases as $|T-T_\lambda|$ increases. Thus the observed $c_{11}{}^S$ should agree quite closely with the predicted behavior of $c_{11}{}^T$. From Fig. 4 we see that the shape of $c_{11}{}^S$ at constant volume is strikingly related to the shape expected from the heat-capacity curve.[24]

[24] F. Simon, Ann. Physik **68**, 4 (1922); C. C. Stephenson (private communication).

Notice also the considerable difference between the shape of the c_{11}-vs-T curve at constant pressure and at constant volume.

Equation (6) would seem to predict that $1/\beta^T$ could become negative near the lambda point (where $C_I \to \infty$). However, the crystal becomes unstable as $1/\beta^T \to 0$ and should undergo a first-order transition. Details of this kind of behavior are given in Paper I, where instability and hysteresis are predicted for an Ising model. Our data indicate that $1/\beta^S$ does not vanish at any temperature, but precise work is very difficult in the critical region due to the extremely high attenuation. In any case, the lack of very accurate thermal expansion and specific heat data in the immediate region of the critical point makes it impossible to calculate $1/\beta^T$ from $1/\beta^S$. Therefore, we do not know whether $1/\beta^T$ vanishes or not. However, the shear constants (especially c_{44}) are sensitive functions of the molar volume and can be viewed as probes to study the behavior of the volume near the lambda point. Since there is no excess attenuation associated with the shear waves, it is possible to follow their behavior throughout the entire transition region both on warming and cooling the sample.

Both c_{44} and C' show a definite hysteresis of $0.9° \pm 0.2°$K at 1 atm, and for c_{44} this has been followed as a function of pressure (see the inset on Fig. 1). In addition, our shear data strongly suggest a sluggish first-order transition in the critical region. For points taken at temperatures more than 1°K away from T_λ and at pressures more than 100 bar away from p_λ, equilibrium was achieved within about 15 min after the temperature or pressure was adjusted. In the immediate vicinity of a critical point, very slow changes in velocity were still observed 45 min after the temperature or pressure was adjusted, as would be expected in a metastable region. Also the changes in c_{44} and C' in this narrow hysteresis region are extremely abrupt, even when compared with the very rapid variations observed in the ordered phase near the transition line. (See Figs. 5 and 6.) The presence of hysteresis and the very abrupt changes in velocities near T_λ are perhaps the most significant features of our shear data at 1 atm.

This same sort of behavior has also been observed in the temperature dependence of the volume of powdered samples of NH_4Cl. Dinichert[25] carried out a very careful x-ray measurement of the unit cell dimensions in the critical region, while Thomas and Staveley[26] measured the volume directly. In both cases, a hysteresis loop was observed with a temperature width of about 0.4°K. At the transition temperature, on cooling and warming, a very sharp volume change of $\Delta V/V = 4.7 \times 10^{-3}$ was observed. Both these authors proposed theories for this hysteresis, which are not discussed here except to point out that both theories treat the transition as first order.

[25] P. Dinichert, Helv. Phys. Acta **15,** 462 (1942).

[26] D. G. Thomas and L. A. K. Staveley, J. Chem. Soc. **1951,** 1420.

The discussion given in Paper I shows how the usual ideas of order–disorder transitions based on Ising models can be reconciled with the notion of a first-order transition and hysteresis. The qualitative behavior of ammonium chloride is in excellent agreement with the predictions of Paper I, and we shall attempt a more quantitative comparison by making an approximate calculation of the hysteresis predicted for a three-dimensional Ising model. Let us begin in terms of the two-dimensional case and refer to Fig. 1 of Paper I. On the Ising isotherm T_5 we have marked the point D where the tangent is parallel to the disordered-lattice isotherm; on the disordered-lattice isotherm T_5 we have marked the point C such that the line DC is parallel to the area axis. We notice that to a rough approximation (valid for a small range of temperatures near the critical point) the Ising isotherms are related to each other by a translation parallel to the σ axis. The same is valid in a more general sense for the disordered-lattice isotherms. In this approximation, all points on the spin isotherms where the tangent is equal to the slope of the disordered-lattice isotherm are on a straight line parallel to the σ axis. If T_5 is the temperature of the upper mechanical instability point, and T_3 is that of the lower one, then $\Delta T = T_5 - T_3$ can be determined from the condition $\sigma_D - (d\sigma_D/dT)\Delta T = \sigma_{3'} = \sigma_C - \sigma_C \alpha_{dl} \Delta T$. This gives

$$\Delta\sigma' = [\sigma_C \alpha_{dl} - (d\sigma_D/dT)]\Delta T,$$

where $\Delta\sigma'$ is defined as $\sigma_C - \sigma_D$. But $d\sigma_D/dT \simeq d\sigma_5/dT$ and σ_C will be numerically quite close to σ_5, therefore

$$\Delta T \simeq \frac{\Delta\sigma'}{\sigma_5} \Big/ \left(\alpha_{dl} - \frac{1}{\sigma_5}\frac{d\sigma_5}{dT}\right). \tag{10}$$

We define also $\Delta\sigma = \sigma_{5'} - \sigma_5$; thus $\Delta\sigma/\sigma_5$ is the relative area expansion of the crystal when the first-order transition takes place on warming. For a three-dimensional crystal, Eq. (10) becomes

$$\Delta T \simeq \frac{\Delta v'}{v_\lambda} \Big/ \left[\alpha_{dl} - \frac{1}{v_\lambda}\left(\frac{dv}{dT}\right)_\lambda\right], \tag{11}$$

and the relative volume change associated with the first-order transition is denoted by $\Delta v/v_\lambda$.

Now we wish to calculate ΔT and $\Delta v/v_\lambda$ for ammonium chloride. We know $(1/v_\lambda)(dv/dT)_\lambda$ experimentally. The value for α_{dl} in the critical region can be extrapolated from the temperature dependence of the thermal expansion in the disordered phase far away from the lambda point. To evaluate $\Delta v'/v_\lambda$ and $\Delta v/v_\lambda$ we use Fisher's theoretical expressions for the specific heat "per site" for a simple-cubic lattice,[27] which are based on an assumed logarithmic singularity at the critical point. Integrating his expressions above and below the critical temperature with respect to $H \equiv J/kT$ we obtain the internal energy "per site" as a function of H. From Eq. (6) of Paper I we get equations for p_I

[27] M. E. Fisher, Phys. Rev. **136,** A1599 (1964).

around the critical point. Using the known variation of T_λ (and thus J) with v, one can plot on a p–V diagram the Ising isotherm at 241.5°K and the disordered-lattice isotherm based on the extrapolated value at 241.5°K of the isothermal compressibility $\beta_{dl}{}^T$. (We used $\beta_{dl}{}^T = 5.9\times10^{-12}$ cm^2 dyn^{-1}.) From this plot we determined $\Delta v/v_\lambda = 0.78\times10^{-3}$ and $\Delta v'/v_\lambda = 1.15\times10^{-4}$. Substituting this latter value into Eq. (11) and letting $(1/v_\lambda)(dv/dT)_\lambda = -4.17\times10^{-4}$ deg^{-1} and $\alpha_{dl} = 1.11\times10^{-4}$ deg^{-1}, we find a hysteresis ΔT of 0.22°K.

The predicted value of $\Delta v/v_\lambda$ (0.78×10^{-3}) is smaller than the experimental value of 4.7×10^{-3}. This could mean that the singularity at the critical temperature is stronger than a logarithmic singularity, which is certainly possible because a logarithmic singularity is the weakest type. However, we must remember that Fisher's expressions are not exact and Eq. (11) involves several approximations; thus we should not expect better than order-of-magnitude agreement. Since the predicted value of $\Delta v/v_\lambda$ is too small, $\Delta v'/v_\lambda$ and ΔT should also be too small. If we use the experimental $\Delta v/v_\lambda$ value as a guide for correcting our prediction of ΔT, a new predicted value of 1.3°K would be obtained. Thus the theoretical maximum value of the temperature hysteresis should lie in the range 0.2° to 1.3°K, in reasonable agreement with the observed values which range between 0.4° and 0.9°K. Although this comparison between theory and experiment is difficult and approximate, it strongly supports the validity of the Ising model defined in Paper I as a description of the ordering process in ammonium chloride.

In summary, we have shown that there is agreement over a wide range of temperatures between the constant-volume elastic constants of NH_4Cl single crystals and the predicted elastic behavior of a compressible Ising model and in addition that the predicted instability and hysteresis at temperatures very close to the lambda point does occur. Ammonium chloride is a favorable case for observing such effects. It is interesting to speculate that the same effects may be present on a much smaller scale near order–disorder points in other, less compressible crystals.